Carbohydrate Polymers 83 (2011) 640–644

Contents lists available at ScienceDirect

Carbohydrate Polymers

journal homepage: www.elsevier.com/locate/carbpol

Polysaccharides as stabilizers for the synthesis of magnetic nanoparticles

Peter R. Chang[b,c], Jiugao Yu[a], Xiaofei Ma[a,*], Debbie P. Anderson[b]

[a] Chemistry Department, School of Science, Tianjin University, Tianjin 300072, China
[b] Bioproducts and Bioprocesses National Science Program, Agriculture and Agri-Food Canada, 107 Science Place, Saskatoon, SK S7N 0X2, Canada
[c] Department of Agricultural and Bioresource Engineering, University of Saskatchewan, Saskatoon, SK, S7N 5A9, Canada

ARTICLE INFO

Article history:
Received 17 July 2010
Received in revised form 10 August 2010
Accepted 12 August 2010
Available online 18 August 2010

Keywords:
Agar
Carboxymethyl cellulose sodium
Fe_3O_4
Starch
Nanoparticles

ABSTRACT

In this study, superparamagnetic Fe_3O_4 nanoparticles were individually prepared with one of three polysaccharides as stabilizer, i.e. soluble starch, carboxymethyl cellulose sodium (CMC) and agar. Since polysaccharides present the dynamic supramolecular associations facilitated by inter- and intramolecular hydrogen bonding, they can act as templates for the growth of nanosized Fe_3O_4. The resultant polysaccharide–Fe_3O_4 were characterized by Fourier transform infrared (FTIR) spectroscopy, thermogravimetric (TG) analysis, transmission electron microscopy (TEM), X-ray diffraction (XRD) and magnetic properties. TEM revealed that Fe_3O_4 was encapsulated by polysaccharides. The particle size of starch–Fe_3O_4 (SF) was obviously smaller than those from CMC–Fe_3O_4 (CF) and agar–Fe_3O_4 (AF). TG analysis was used to calculate the Fe_3O_4 contents of SF, CF and AF—62.7, 47.8 and 57.4%, respectively. The saturation magnetization (20.43 emu/g) of AF was much lower than that of SF (36.16 emu/g) and CF (35.75 emu/g). The polysaccharide–Fe_3O_4 exhibited an extremely small hysteresis loop and low coercivity.

© 2010 Elsevier Ltd. All rights reserved.

1. Introduction

During the past decade, remarkable progress has been made in the use of natural polysaccharides for controlling inorganic crystal nucleation and growth. Carboxymethyl chitosan has been reported to stabilize nanoparticles of platinum, gold, and silver (Laudenslager, Schiffman, & Schauer, 2008). Raveendran, Fu, and Wallen (2003) used soluble starch as the template and β-D-glucose as the reductant in an aqueous solution of $AgNO_3$ for the growth of silver nanoparticles. Arabinogalactan (Mucalo, Bullen, Manley-Harris, & McIntire, 2002) and porous cellulose fibers (He, Kunitake, & Nakao, 2003) served as novel stabilizers for maintaining metal (platinum, palladium and silver) nanoparticles in colloidal suspension. Walsh, Arcelli, Ikoma, Tanaka, and Mann (2003) prepared self-supporting macroporous sponges of silver, gold and copper oxide, as well as composites of silver/copper oxide or silver/titania by heating dextran/metal salt mixtures where dextran served as the soft template. Recently, nanoparticles of metal oxide and sulfides were also prepared with starch as the stabilizer. Zinc oxide nanoparticles were synthesized using water as the solvent and soluble starch as the stabilizer (Ma, Chang, Yang, & Yu, 2009; Vigneshwaran, Kumar, Kathe, Varadarajan, & Prasad, 2006), while CdS nanoparticles were synthesized in a sago starch matrix (Radhakrishnan, Georges, Nair, Luyt, & Djokovic, 2007). Silver (Ag) and silver sulfide (Ag_2S) nanoparticles have also been fabricated in a sago starch matrix (Bozanic et al., 2007). Carboxymethyl cellulose sodium was used as the stabilizer in preparation of Sb_2O_3 and ZnO nanoparticles (Chang, Yu, & Ma, 2009; Yu, Yang, Liu, & Ma, 2009).

Magnetic iron oxide (Fe_3O_4) nanoparticles have a wide variety of applications in physics, medicine, biology and material science due to their small size, superparamagnetism, low toxicity, etc. Many stabilizers, including solvents such as hexane and decane (Fried, Shemer, & Markovich, 2001; Shafi et al., 2001); water-in-oil microemulsions formed from non-ionic surfactants (Santra et al., 2001); and polymers (Matsuno, Yamamoto, Otsuka, & Takahara, 2004), have been used to modify these nanoparticles to increase their stability. However, the poor solubility of these stabilizers in aqueous solutions restricts their biological applications. Biocompatible chitosan and carboxymethyl chitosan were effective dispersants used in the preparation of the well-dispersed suspension of magnetic Fe_3O_4 nanoparticles (Zhu, Yuan, & Liao, 2008). Li, Jiang, Huang, Ding, and Chen (2008) fabricated Fe_3O_4–chitosan nanoparticles by covalent binding of chitosan to the Fe_3O_4 nanoparticles.

In this paper, three polysaccharides (soluble starch, carboxymethyl cellulose sodium and agar) were used individually as stabilizers during the synthesis of magnetic Fe_3O_4 nanoparticles in order to improve the stability, biocompatibility and biodegradability. Agar is composed of a disaccharide-repeating units of 1,3-linked-D-galactose and 1,4-linked 3, 6-anhydro-L-galactose with the possible occurrence of sulfate, methoxyl, and/or pyruvate substituents at various positions in the polysaccharide chain (Villanueva, Sousa, Goncalves, Nilsson, & Hilliou, 2010). This work is

* Corresponding author. Tel.: +86 22 27406144; fax: +86 22 27403475.
E-mail address: maxiaofei@tju.edu.cn (X. Ma).

0144-8617/$ – see front matter © 2010 Elsevier Ltd. All rights reserved.
doi:10.1016/j.carbpol.2010.08.027

focused on the preparation of the polysaccharide–Fe_3O_4 nanoparticles and characterization of them using FTIR spectroscopy, transmission electron microscopy, X-ray diffractometry, thermogravimetric analysis, and testing of magnetic properties.

2. Materials and methods

2.1. Materials

Soluble starch, carboxymethyl cellulose sodium (CMC) and agar were obtained from Tianjin Fine Chemical Institute (Tianjin, China). The reagents, including $FeCl_3{\cdot}6H_2O$, $FeSO_4{\cdot}7H_2O$, NH_3H_2O and ethanol were of analytical grade from Tianjin Chemical Reagent Factory (Tianjin, China).

2.2. Preparation of starch–Fe_3O_4 (SF), CMC–Fe_3O_4 (CF) and agar–Fe_3O_4 (AF)

A quantity of 1.2 g of polysaccharide (soluble starch, CMC, or agar) was added to 200 ml distilled water. The mixture was heated at 90 °C for about 10 min with constant stirring for dissolution of the polysaccharide. The solution was subsequently cooled to the room temperature. $FeCl_3{\cdot}6H_2O$ (1.49 g) and $FeSO_4{\cdot}7H_2O$ (0.765 g) were added to the solution, which was then heated at 60 °C under nitrogen. An ammonia–water solution (8 mol l^{-1}) was added dropwise and a suspension was obtained. The pH of the final mixture was controlled in the range of 10–11. The mixtures were held at 60 °C for 4 h and the suspension was then centrifuged at 12,000 rpm for 10 min. The settled polysaccharide–Fe_3O_4 was washed three times using distilled water to remove by-products and excess polysaccharides. The polysaccharide–Fe_3O_4 particles were then washed two times with distilled water and then with ethanol. The obtained hybrids were dried in an oven at 100 °C for 3 h and labelled as SF, CF, and AF, respectively.

2.3. Fourier transform infrared (FTIR) spectroscopy

FTIR analysis of soluble starch, CMC, agar, SF, CF and AF particles was performed at 2 cm^{-1} resolution in transmission mode on a BIO-RAD FTS3000 IR Spectrum Scanner. Typically, 64 scans were signal-averaged to reduce spectral noise.

2.4. X-ray diffractometry (XRD)

The SF, CF and AF particles were tightly packed into the sample holder and X-ray diffraction patterns were recorded in the reflection mode at ambient temperature by a BDX3300 diffractometer, operated at a Cu Kα wavelength of 1.541 Å. Radiation from the anode operated at 36 kV and 20 mA, monochromized with a 15 μm nickel foil. The diffractometer was equipped with a 1° divergence slit, 16 mm beam bask, 0.2 mm receiving slit, and a 1° scatter slit. Radiation was detected with a proportional detector.

2.5. Thermogravimetric (TG) analysis

The thermal properties of soluble starch, CMC, agar, SF, CF and AF were measured with a ZTY-ZP type thermal analyzer. Sample weights varied from 5 to 10 mg. Samples were heated in Al_2O_3 pans from room temperature to 600 °C at a heating rate of 15 °C/min in a nitrogen atmosphere with a flow rate of 30 ml/min.

2.6. Transmission electron microscopy (TEM)

The suspensions of SF, CF and AF particles in ethanol were dropped onto copper grids and air dried. TEM was performed using a TEM JEM-1200EX.

2.7. Magnetic properties

The magnetic properties of SF, CF and AF were measured at 300 K on a vibrating sample magnetometer LDJ 9600-1 with the magnetic field set at 1.0 T.

3. Results and discussion

3.1. FTIR

As shown in Fig. 1, in the fingerprint region of the soluble starch there were three peaks characteristic of –C–O– stretching. The peak at 1156 cm^{-1} was ascribed to C–O bond stretching of the C–O–H group, and the two peaks at 1080 and 1020 cm^{-1} were attributed to C–O bond stretching of the C–O–C group in the anhydroglucose ring (Ma et al., 2009). In FTIR spectra of SF, there was a high intensity broad band at around 590 cm^{-1}, due to the Fe_3O_4 peak (Luo, Liu, Zhou, & Zhang, 2009). The –C–O– stretching peaks of soluble starch shifted in the presence of Fe_3O_4 indicating that an interaction existed between the starch and Fe_3O_4 in SF, but no obvious covalent bonds were formed (Laudenslager et al., 2008).

In the FTIR spectra of CMC and agar, the absorption bands between 1000 and 1200 cm^{-1} were characteristic of –C–O– stretching on a polysaccharide skeleton. In the CMC FTIR spectra, the two peaks appearing at 1410 and 1610 cm^{-1} corresponded to the symmetrical and asymmetrical stretching vibrations of the carboxylate groups (Rosca, Popa, Lisa, & Chitanu, 2005), while in the agar FTIR spectra, the peak at 1640 cm^{-1} was due to stretching of the conjugated peptide bond formed by amine (NH) and acetone (CO) groups (Freile-Pelegrin et al., 2007). The above-mentioned peaks of CMC and agar also shifted and the characteristic peak of Fe_3O_4 at 590 cm^{-1} appeared in FTIR spectra of CF and AF, indicating that there was an interaction between Fe_3O_4 and CMC (or agar).

3.2. TG

The thermogravimetric (TG) and derivative thermogravimetric (DTG) curves of the polysaccharides and polysaccharide–Fe_3O_4 are shown in Fig. 2. As revealed by the DTG curves, all of the polysaccharides exhibited a peak at about 300 °C, i.e. the temperature at maximum rate of mass loss. The mass loss before the onset temperature was related to the volatilization of water contained in the polysaccharides (Chang, Jian, Yu, & Ma, 2010). The temperature ranges, where the peaks of DTG curves located, were the decomposition temperatures of soluble starch, CMC, and agar. It was

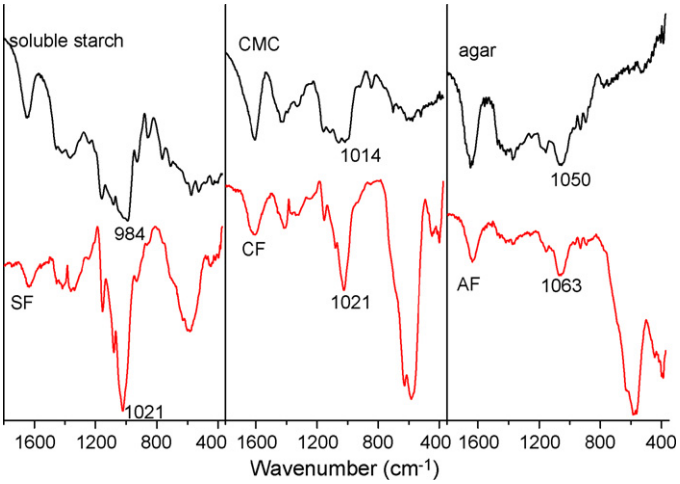

Fig. 1. FTIR spectra of soluble starch, SF, CMC, CF, agar and AF.

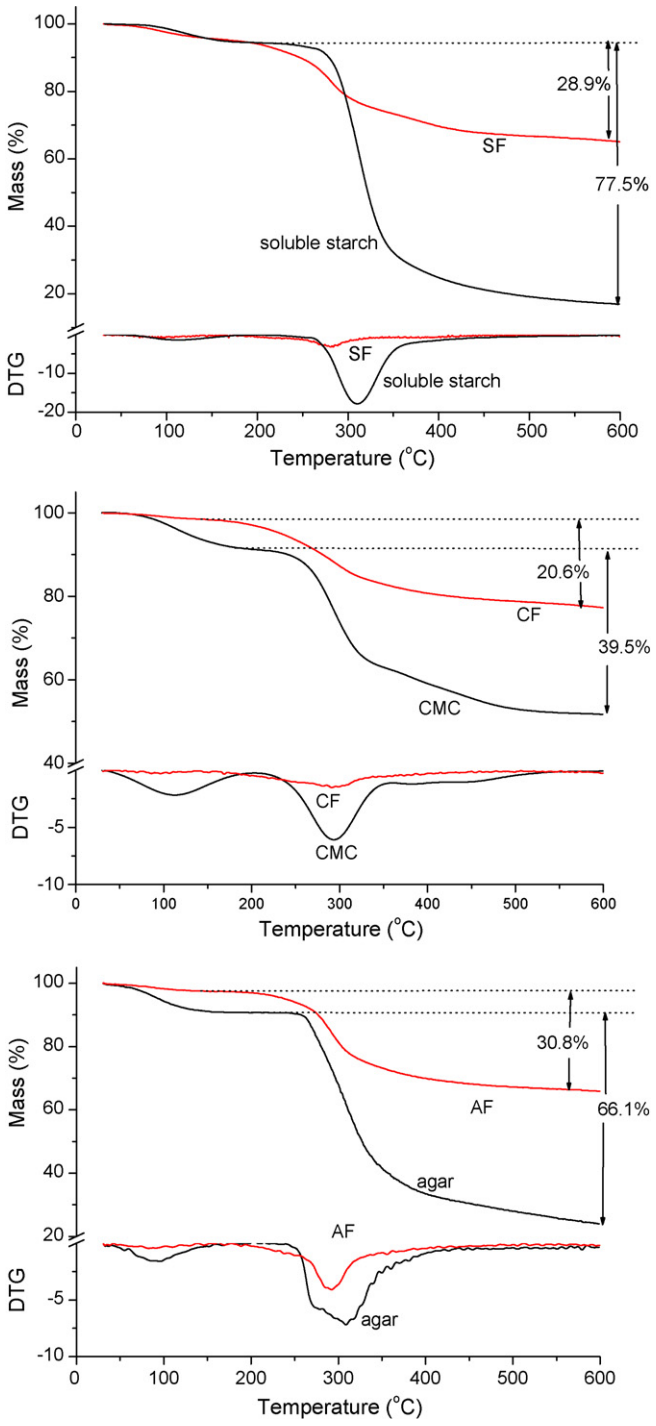

Fig. 2. TG and DTG curves of soluble starch, SF, CMC, CF, agar and AF.

assumed that the percentages of mass loss of the polysaccharides, revealed by TG curves, were constant in the decomposition temperature range when Fe_3O_4 was incorporated with the polysaccharide. The content of the polysaccharide in polysaccharide–starch could be calculated by matching the percentage of mass loss of the polysaccharide–Fe_3O_4 to the percentage of mass loss of the polysaccharide at the decomposition temperature. For example, when the mass loss of SF (28.9%) was divided by the mass loss of soluble starch (77.5%) at the decomposition temperature of soluble starch, the content of soluble starch was estimated to be about 37.3%; therefore, the Fe_3O_4 content of SF was 62.7%. The Fe_3O_4 contents of CF and AF were similarly calculated to be 47.8 and 57.4%, respectively.

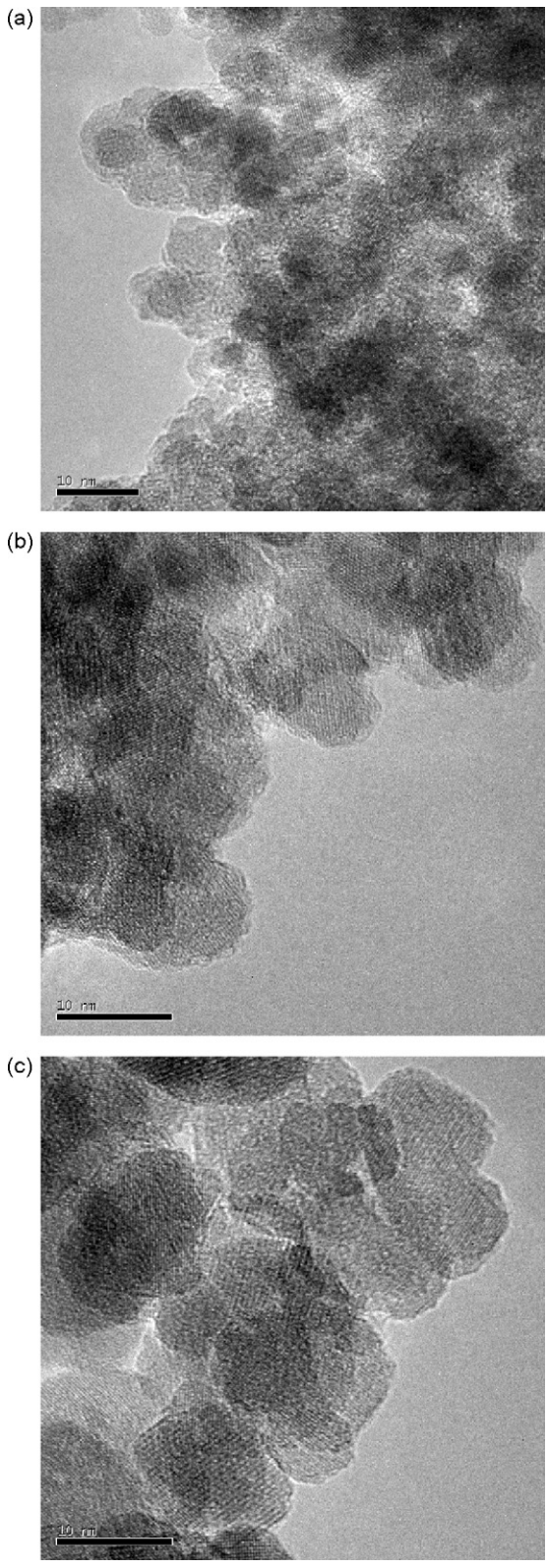

Fig. 3. TEM micrographs for SF (a), CF (b) and AF (c).

3.3. TEM

The central black spot and the light-colored edge shown in Fig. 3 represent Fe_3O_4 nanoparticles and polysaccharides, respectively, clearly showing that the Fe_3O_4 nanoparticles were encapsulated by polysaccharides. Since polysaccharides could form hybrids with

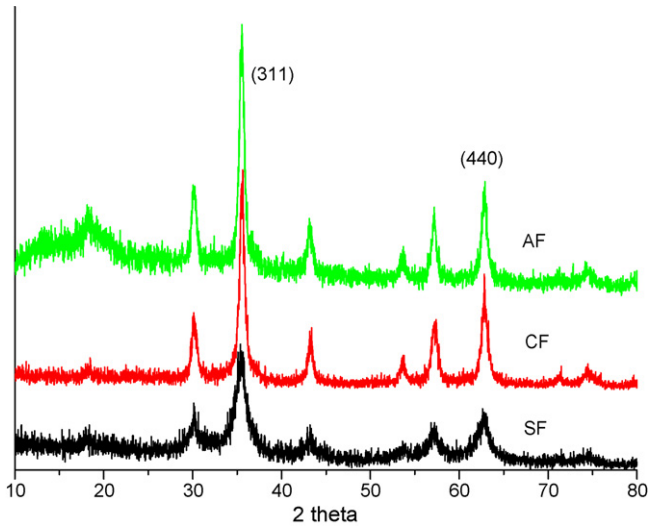

Fig. 4. X-ray diffraction patterns of SF, CF and AF.

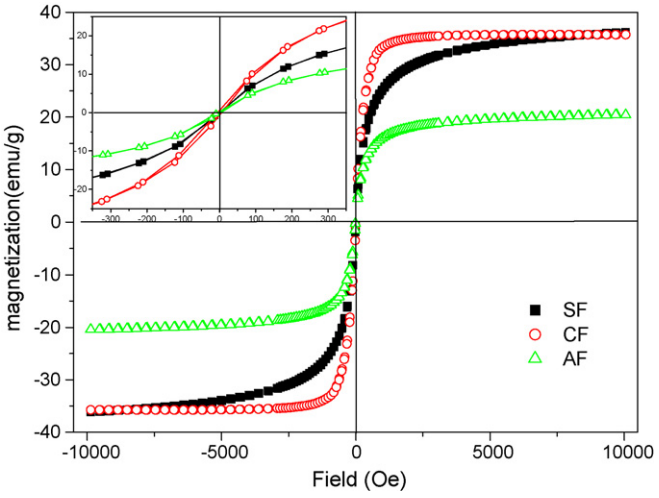

Fig. 5. Magnetization curves of SF, CF and AF at 300 K. Insert: magnified view of the −350 to 350 Oe regions.

metal ions, due to their high number of coordinating functional groups (hydroxyl and glucoside groups) (Taubert & Wegner, 2002), it was likely that the majority of the iron ions was closely associated with the polysaccharide molecules; therefore nucleation and initial crystal growth of Fe_3O_4 may have occurred preferentially on polysaccharides. In addition, polysaccharides present interesting dynamic supramolecular associations facilitated by inter- and intra-molecular hydrogen bonding, which could act as templates for the growth of nanoparticles (Raveendran et al., 2003). SF nanoparticles exhibited an approximately spherical morphology with a mean size of less than 10 nm, while CF and AF nanoparticles were larger. This may be related to the polysaccharide structures; soluble starch is mainly composed of branched amylopectin, while CMC and agar contain a more linear-polysaccharide structure in aqueous solution. As the template, soluble starch formed more interactions with iron ions than did CMC and agar, which exerted more restriction on the growth of Fe_3O_4 particles.

3.4. XRD

As seen in Fig. 4, there was no obvious difference among the XRD patterns of SF, CF and AF particles. The powder XRD patterns (Fig. 4) also displayed distinct peaks at 2θ values of about 18.2, 30.1, 35.5, 43.1, 57.2 and 62.9. These peak positions and relative peak intensities corresponded to the characteristic peaks of Fe_3O_4 (Zhou et al., 2009); therefore, it was determined that magnetic Fe_3O_4 nanoparticles were successfully fabricated in SF, CF and AF. The diffraction peaks of SF showed wider FWHM (full width at half-maximum) than both CF and AF. According to peak search reports of the XRD pattern, FWHM of XRD peaks (3 1 1) for SF, CF and AF were 0.736, 0.615 and 0.586, respectively, and FWHM of (4 4 0) peaks showed the same order, i.e. 0.777, 0.552 and 0.516. The crystallite sizes could be calculated from FWHM using Scherrer's formula (Yu et al., 2009), expressed as $D = 0.89\lambda/(\beta \cos\theta)$, where λ is the wavelength (Cu Kα), β is FWHM of the XRD peaks and θ is the diffraction angle. The Fe_3O_4 nanoparticles in SF were obviously smaller than CF and AF, and this was consistent with the TEM results. Since no obvious crystallinity of the polysaccharide was observed, the polysaccharide component was in the amorphous phase, which could improve the hydrophilicity of the polysaccharide–Fe_3O_4.

3.5. Magnetic properties

The magnetization of Fe_3O_4 is very sensitive to the microstructure. When the Fe_3O_4 particles are smaller than the critical size, they are called single-domain particles. As the particle size continues to decrease below the critical single-domain size, the particles exhibit superparamagnetic properties. However, when the magnetizations of the particles are random, without a fixed direction, each particle suppresses the exchange interaction between the particles. This lack of hysteresis is one of the criteria requirements for identification of a product with superparamagnetic attributes (Zhu et al., 2008).

Fig. 5 shows the magnetization of SF, CF and AF as a function of the applied magnetic field at 300 K. Magnetization increased with an increase in the magnetic field. The saturation magnetism (σ_s) was 36.16 emu/g, remanence (σ_r) was 0.05 emu/g, and the coercivity (H_c) was 0.589 Oe for SF; σ_s was 35.75 emu/g, σ_r was 0.63 emu/g, and H_c was 5.64 Oe for CF; and for AF σ_s was 20.43 emu/g, σ_r was 0.22 emu/g and H_c was 3.78 Oe. SF exhibited an extremely small hysteresis loop and low coercivity, which was typically characteristic of superparamagnetic particles. In the case of CF and AF, both exhibited larger hysteresis loops and coercivity, further confirming that the Fe_3O_4 particle size of SF was smaller than those of CF and AF (Liu et al., 2008). This was also consistent with the findings from TEM and XRD. As a conventional magnet for magnetic separation, SA, CF and AF possessed reasonably good saturation magnetization, although the saturation magnetization (20.43 emu/g) of AF was much lower than that of SF (36.16 emu/g) and CF (35.75 emu/g). Polysaccharide–Fe_3O_4 with superparamagnetic properties would therefore be promising in biological engineering and biomedical applications.

4. Conclusions

Polysaccharide–Fe_3O_4 was obtained by synthesizing Fe_3O_4 particles in polysaccharide aqueous solutions. Soluble starch, CMC and agar played very important roles in the synthesis of Fe_3O_4 nanoparticles. As evidenced from FTIR, good interaction between Fe_3O_4 and polysaccharide functional groups controls the Fe_3O_4 crystal growth. The Fe_3O_4 contents of SF, CF and AF were calculated as 62.7, 47.8 and 57.4%, respectively. TEM and XRD confirmed that SF exhibited a smaller size than CF and AF. In addition, SA, CF and AF possessed reasonably good saturation magnetization, although CF and AF had slightly larger hysteresis loops and coercivity.

Using the technique described in this study, first and foremost, polysaccharide (starch, CMC, agar, chitosan, and so on) films can be enforced with magnetic properties, because the hybrid can form interfacial interactions with other hydrophilic matrices.

Secondly, the hybrid can be incorporated into porous polysaccharide materials for the removal of hazardous substances by magnetic separation. Many interesting and potential applications for polysaccharide–Fe_3O_4 nanoparticles are to be further explored.

References

Bozanic, D. K., Djokovic, V., Blanusa, J., Nair, P. S., Georges, M. K., & Radhakrishnan, T. (2007). Preparation and properties of nano-sized Ag and Ag_2S particles in biopolymer matrix. *The European Physical Journal E*, *22*, 51–59.

Chang, P. R., Jian, R. J., Yu, J. G., & Ma, X. F. (2010). Fabrication and characterization of chitosan nanoparticles/plasticized-starch composites. *Food Chemistry*, *120*, 736–740.

Chang, P. R., Yu, J. G., & Ma, X. F. (2009). Fabrication and characterization of Sb_2O_3/carboxymethyl cellulose sodium and the properties of plasticized starch composite films. *Macromolecular Materials and Engineering*, *294*, 762–767.

Freile-Pelegrin, Y., Madera-Santana, T., Robledo, D., Veleva, L., Quintana, P., & Azamar, J. A. (2007). Degradation of agar films in a humid tropical climate: Thermal, mechanical, morphological and structural changes. *Polymer Degradation and Stability*, *92*, 244–252.

Fried, T., Shemer, G., & Markovich, G. (2001). Ordered two-dimensional arrays of ferrite nanoparticles. *Advanced Materials*, *13*, 1158–1161.

He, J. H., Kunitake, T., & Nakao, A. (2003). Facile in situ synthesis of noble metal nanoparticles in porous cellulose fibers. *Chemistry of Materials*, *15*, 4401–4406.

Laudenslager, M. J., Schiffman, J. D., & Schauer, C. L. (2008). Carboxymethyl chitosan as a matrix material for platinum, gold, and silver nanoparticles. *Biomacromolecules*, *9*, 2682–2685.

Li, G. Y., Jiang, Y. R., Huang, K. L., Ding, P., & Chen, J. (2008). Preparation and properties of magnetic Fe_3O_4–chitosan nanoparticle. *Journal of Alloys and Compounds*, *466*, 451–456.

Liu, S. L., Zhang, L. N., Zhou, J. P., Xiang, J. F., Sun, J. T., & Guan, J. G. (2008). Fiberlike Fe_2O_3 macroporous nanomaterials fabricated by calcinating regenerate cellulose composite fibers. *Chemistry of Materials*, *20*, 3623–3628.

Luo, X. G., Liu, S. L., Zhou, J. P., & Zhang, L. N. (2009). In situ synthesis of Fe_3O_4/cellulose microspheres with magnetic-induced protein delivery. *Journal of Materials Chemistry*, *19*, 3538–3545.

Ma, X. F., Chang, P. R., Yang, J. W., & Yu, J. G. (2009). Preparation and properties of glycerol plasticized-pea starch/zinc oxide-starch bionanocomposites. *Carbohydrate Polymers*, *75*, 472–478.

Matsuno, R., Yamamoto, K., Otsuka, H., & Takahara, A. (2004). Polystyrene- and poly(3-vinylpyridine)-grafted magnetite nanoparticles prepared through surface-initiated nitroxide-mediated radical polymerization. *Macromolecules*, *37*, 2203–2209.

Mucalo, M. R., Bullen, C. R., Manley-Harris, M., & McIntire, T. M. (2002). Arabinogalactan from the Western larch tree: A new, purified and highly water-soluble polysaccharide-based protecting agent for maintaining precious metal nanoparticles in colloidal suspension. *Journal of Materials Science*, *37*, 493–504.

Radhakrishnan, T., Georges, M. K., Nair, P. S., Luyt, A. S., & Djokovic, V. (2007). Study of sago starch–CdS nanocomposite films: Fabrication, structure, optical and thermal properties. *Journal of Nanoscience and Nanotechnology*, *7*, 986–993.

Raveendran, P, Fu, J., & Wallen, S. L. (2003). Completely "green" synthesis and stabilization of metal nanoparticles. *Journal of the American Chemical Society*, *125*, 13940–13941.

Rosca, C., Popa, M. I., Lisa, G., & Chitanu, G. C. (2005). Interaction of chitosan with natural or synthetic anionic polyelectrolytes. 1. The chitosan–carboxymethyl–cellulose complex. *Carbohydrate Polymers*, *62*, 35–41.

Santra, S., Tapec, R., Theodoropoulou, N., Dobson, J., Hebard, A., & Tan, W. H. (2001). Synthesis and characterization of silica-coated iron oxide nanoparticles in microemulsion: The effect of non-ionic surfactants. *Langmuir*, *17*, 2900–2908.

Shafi, K. V. P. M., Ulman, A., Yan, X., Yang, N. L., Estournes, C., White, H., et al. (2001). Sonochemical synthesis of functionalized amorphous iron oxide nanoparticles. *Langmuir*, *17*, 5093–5097.

Taubert, A., & Wegner, G. (2002). Formation of uniform and monodisperse zincite crystals in the presence of soluble starch. *Journal of Materials Chemistry*, *12*, 805–807.

Vigneshwaran, N., Kumar, S., Kathe, A. A., Varadarajan, P. V., & Prasad, V. (2006). Functional finishing of cotton fabrics using zinc oxide-soluble starch nanocomposites. *Nanotechnology*, *17*, 5087–5095.

Villanueva, R. D., Sousa, A. M. M., Goncalves, M. P., Nilsson, M., & Hilliou, L. (2010). Production and properties of agar from the invasive marine alga, Gracilaria vermiculophylla (Gracilariales, Rhodophyta). *Journal of Applied Phycology*, *22*, 211–220.

Walsh, D., Arcelli, L., Ikoma, T., Tanaka, J., & Mann, S. (2003). Dextran templating for the synthesis of metallic and metal oxide sponges. *Nature Materials*, *2*, 386–390.

Yu, J. G., Yang, J. W., Liu, B. X., & Ma, X. F. (2009). Preparation and characterization of glycerol plasticized-pea starch/ZnO-carboxy-methylcellulose sodium nanocomposites. *Bioresource Technology*, *100*, 2832–2841.

Zhou, J. P., Li, R., Liu, S. L., Li, Q., Zhang, L. Z., Zhang, L. N., et al. (2009). Structure and magnetic properties of regenerated cellulose/Fe_3O_4 nanocomposite films. *Journal of Applied Polymer Science*, *111*, 2477–2484.

Zhu, A. P., Yuan, L. H., & Liao, T. Q. (2008). Suspension of Fe_3O_4 nanoparticles stabilized by chitosan and *o*-carboxymethyl chitosan. *International Journal of Pharmaceutics*, *350*, 361–368.